



# Comparative study of electrically conductive cotton fabric prepared through the in situ synthesis of different conductive materials

Hossein Barani · Adel Miri · Hassan Sheibani

Received: 28 October 2020 / Accepted: 6 May 2021 / Published online: 17 May 2021  
© The Author(s), under exclusive licence to Springer Nature B.V. 2021

**Abstract** The electrical conductivity of cotton fabrics was enhanced using an in situ synthesis of graphene or polymerization of conductive polymer. The impact of conductive materials concentration and monomer to oxidant molar ratio examined on the sheet resistance of coated cotton fabric. The polypyrrole coating resulted in a continuous layer consisting of spherical particles of different sizes, which presented an excellent electrical conductivity. The FTIR spectroscopy showed successful production of synthesized conductive materials. The ATR–FTIR spectroscopy confirmed hydrogen bonds between the hydroxyl groups of cotton fibers and the conductive materials. The successful exfoliation and uniform deposition of graphene over the fibers were verified by the crystallographic structure of the graphene-coated cotton fabric. The deposition of graphene oxide resulted in

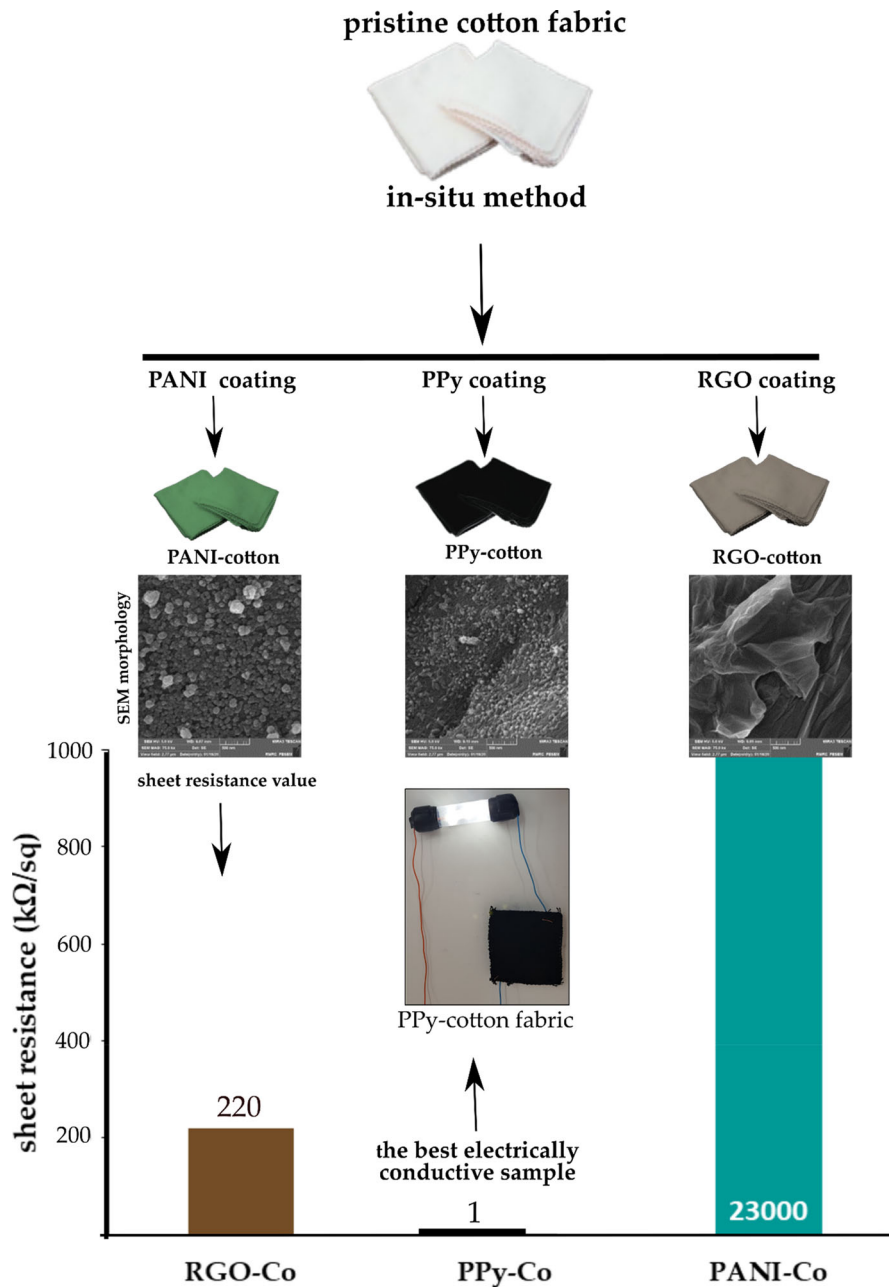
a partial decrease in the electrical resistance of the cotton sample. However, reduced graphene oxide showed a sheet resistance of  $220 \times 10^3 \Omega/\text{square}$ , representing a decrease of 95%. The lowest sheet resistance of  $1 \times 10^3 \Omega/\text{square}$  was observed in the polypyrrole coated cotton, and the pyrrole to oxidant molar ratio didn't affect the conductivity of the coated cotton fabric. In contrast, the sheet resistance of polyaniline-coated cotton fabrics depended on the molar ratio of aniline to oxidant. Also, the electrical conductivity of synthesized polyaniline is very sensitive to the degree of oxidation and protonation. The protonated pernigraniline altered to green color due to the emeraldine salt and showed the lowest sheet resistance.

---

H. Barani (✉)  
Department of Carpet, University of Birjand, 17 Shahrivar  
Street, Birjand, Iran  
e-mail: barani@birjand.ac.ir

A. Miri · H. Sheibani (✉)  
Department of Chemistry, Shahid Bahonar University of  
Kerman, 76169 Kerman, Iran  
e-mail: hsheibani@uk.ac.ir

## Graphic abstract



**Keywords** Cotton fabric · Electrical conductivity · Sheet resistance · Conductive polymer · Polypyrrole · Polyaniline

### Introduction

Cotton as a natural polysaccharide is a quite popular fiber. It is generally employed in the daily life and textile industry according to the outstanding properties, such as softness, skin-friendliness, sweat absorbing properties, high breathability, and hygroscopicity.

However, the fabric production with new functionalities, including antibacterial properties (Barani and Mahltig 2020), self-cleaning (Karimi et al. 2014), thermal regulation (Peng et al. 2019), flame resistance (Gao et al. 2015; Yang et al. 2016), and electrical properties (Ahmed et al. 2020; Alamer 2018; Karimi et al. 2014; Wang et al. 2017; Yang et al. 2018; Zhou et al. 2020) has received a great deal of interest during the recent years. Among these properties, the production of conductive textiles has attracted specific attention due to the intrinsic properties, such as lightweight and flexibility. Conductive textile represents a novel type of textile, which is known as smart textile or E-textile. This type of textile demonstrates several applications such as antibacterial fabrics (Karimi et al. 2014; Zhao et al. 2019), electromagnetic shielding (Bharadiya et al. 2019; Wang et al. 2017), flexible energy storage (He et al. 2019a, b; Ke and Wang 2016), digital component electronics (Matsuhisa et al. 2015), and wearable sensing in biomechanical monitoring (Xue et al. 2020). This product is constructed based on the embedding of conductive materials such as conductive polymers and nanomaterials of metals and alloys on the textile substrate (Al-Oqla et al. 2015). Nylon, polyester, and cotton textiles have been made electroconductive using different methods (Ahmed et al. 2020; Alamer 2018; Karimi et al. 2014; Kongahge et al. 2016; Lou et al. 2017; Wang et al. 2017; Yang et al. 2018; Yue et al. 2012; Zhou et al. 2020), such as insert of metallic fibers in the fabric, the extrusion of fibers with conductive particles, or coating of the textile substrate with conducting polymer or chemical metallization.

Graphene is a unique class of carbon-based nanoscale building blocks that presents a considerable potential for energy conversion and storage devices (Kongahge et al. 2016; Lou et al. 2017; Yu et al. 2011). The graphene is a two-dimensional sheet of  $sp^2$  hybridization carbon atoms that recently attained a great research interest according to its unique properties, such as good flexibility, high mechanical strength, and high electrical and thermal conductivity. Graphene oxide (GO) is an oxidized form of graphene that contains a variety of oxygen functional groups such as hydroxyl, carbonyl, carboxyl, and epoxy groups on the basal plane and the edges (Kongahge et al. 2016; Wong et al. 2015; Zhou et al. 2011). These functional groups provide the dispersal ability of the synthesized GO nanosheets in water and enhance their binding to

cotton fibers surface. However, its electronic applications are limited due to the low conductivity caused by the  $sp^2$  bonding network disruption. Therefore, the partial reduction of GO nanosheets is favorable for increasing electroconductivity. Different methods are used to reduce the deposited GO on the textile substrates, including chemical reduction based on various reducing agents and thermal reduction. In these methods, the GO nanosheets were adsorbed on the surface of the textile substrate and later reduced by employing chemical reducing agents such as hydro-sulfite (Pei and Cheng 2012; Zhou et al. 2011) or hydrazine (Gholampour et al. 2017; Park et al. 2011). The GO nanosheets were adsorbed on the surface of the fabric due to the presence of chemical attraction forces between the extent of the oxidized groups of GO and functional groups of the textile substrates. Yu et al. coated the solution-exfoliated graphene nanosheets on polyester fabric and later electrodeposited manganese dioxide ( $MnO_2$ ) to yield high-capacitance performance (Yu et al. 2011).

Conducting polymers are materials capable of being doped or undoped, resulting in changes to their electrical properties. Recently, the conductive polymers with conjugated double bonds have gained popularity in advanced materials (Bhadra et al. 2020; Kaur et al. 2015; Palza et al. 2019; Tian et al. 2014). A large variety of conducting electroactive polymers have been reported in the literature, some of which are polypyrrole (PPy), polythiophene (PTh), and polyaniline (PANI) (Ansari 2006; Balint et al. 2014; Boeva and Sergeev 2014; Wallace et al. 2008). Polypyrrole is the most intensively investigated conducting polymer owing to its high stability and ease of tailoring to prepare functionalized polypyrrole (Ansari 2006). Polypyrrole can be polymerized using either chemical or electrochemical methods (Machida et al. 1989; Muthulakshmi et al. 2006). The polyaniline family includes the unsubstituted “parent” polyaniline and various substituted polymers with substituents either on the aniline rings or on the nitrogen atoms. Polypyrrole and polyaniline can be coated on the textile to form conducting polymer textiles using various methods for this purpose. The electrically conductive coating must be uniform, smooth, and bonded covalently to the fiber surface for presenting excellent stability against high friction forces and extreme bending radii (Allison et al. 2017; He et al. 2019a, b; Zhao et al. 2017). Depending on the

presence/absence of reactive functional groups on the surface of fibers, reactive monomers or growing polymer chains can also become covalently attached to the surface of fibers during the coating (David et al. 2017; Xie et al. 2019). The most commonly used methods are chemical polymerization (in situ polymerization) (Butoi et al. 2017; Machida et al. 1989; Malinauskas 2001; Yue et al. 2012) or electrochemical polymerization (Muthulakshmi et al. 2006; Yue et al. 2012, 2013). In general, it can be stated that the in situ polymerization of conductive polymers on textile substrate generated a homogeneous layer with higher conductivity and better rubbing fastness compared to material coated via dipping and drying. In an in situ polymerization process, pyrrole or aniline monomer is usually chemically polymerized from solution and deposited onto the textile's surface. The monomer's oxidation must be maintained slow for obtaining uniform coating on a textile substrate (Higashimura 2012; Le et al. 2017; Patil and Deogaonkar 2012). It is achieved by controlling the concentration of both monomer and oxidant. The in situ polymerization of pyrrole was first used on the paper by Bjorklund (Shea 1999) and later was developed for textile (Butoi et al. 2017; Machida et al. 1989; Malinauskas 2001; Muthulakshmi et al. 2006; Yue et al. 2012, 2013). It has been found that either pyrrole or aniline monomers could be polymerized onto the textile and forms a smooth, coherent coating on the textile materials' surface.

Some studies have been done on the preparation of conductive cotton fabric based by applying several types of conductive materials, including graphene and conductive polymers. Despite these several methods, the modification and development of new methods for producing electrically conductive cotton fabric remain a considerable challenge. The present paper aims to enhance the electrical conductivity of cotton fabrics based on using different conductive materials with an in situ approach. To the best of our knowledge, there is no reported literature regarding comparing the prepared conductive textile substrate using different preparation methods and conductive materials. Comparing the electrical conductivity of prepared cotton fabric with various conductive materials such as RGO, polypyrrole, or polyaniline is the main purpose of the current work. Moreover, the effect of different concentrations of conductive materials, monomer to oxidant, and monomer to dopant molar ratios was

examined on the sheet resistance of coated cotton fabric. The sulfur-containing compounds such as  $\text{NaHSO}_3$ ,  $\text{Na}_2\text{SO}_3$ , and  $\text{Na}_2\text{S}_2\text{O}_4$  are newly found as reducing agents. Besides higher conductivity, due to the low toxicity and nonvolatility, these materials make the reduction much safer (Chen et al. 2010). Therefore,  $\text{Na}_2\text{S}_2\text{O}_4$  was used to reduce GO to graphene in this study. The influence of conductive material types, material concentrations, and polymerization conditions was investigated on the morphology, color characteristic, and sheet resistance of produced conductive cotton fabric.

## Experimental

### Materials

Graphite powder, particle size averages of less than 100  $\mu\text{m}$ , was purchased from Fluka chemical company. Sulfuric acid ( $\text{H}_2\text{SO}_4$ , 95–98%) and hydrochloric acid (HCl, 32%) were acquired from the Kian Kaveh Azma chemical company (Iran). Potassium permanganate ( $\text{KMnO}_4$ ), sodium nitrate ( $\text{NaNO}_3$ ), hydrogen peroxide ( $\text{H}_2\text{O}_2$ , 37%), sodium hydrosulfite ( $\text{Na}_2\text{S}_2\text{O}_4$ ), iron (III) chloride hexahydrate ( $\text{FeCl}_3 \cdot 6\text{H}_2\text{O}$ ), ammonium persulfate (APS,  $(\text{NH}_4)_2\text{S}_2\text{O}_8$ ), pyrrole (Py) were purchased from Merck chemical company (Germany). Aniline (Ani) was supplied by Acros organics Company (Germany). Nonionic surfactant Triton X-100 was acquired from Biochemica Company (United Kingdom). Pyrrole and Aniline were freshly distilled, whereas other chemicals were used as a received. The 100% cotton fabrics (scoured and bleached sample) with a plain weave structure were used as a substrate. The structural characteristic of used cotton fabric in this assay is as follows: fabric density, 143  $\text{g}/\text{m}^2$ ; warp threads per cm, 27; weft threads per cm, 20. The purified water with a resistivity higher than 18.2  $\text{M}\Omega/\text{cm}$  (Milli-Q system) was used in all experiments.

### Preparation of electrically conductive cotton fabric

In this study, the electrical conductivity of cotton fabric was enhanced based on the in situ polymerization of conductive polymer and the coating with synthesized GO and the RGO. Therefore, different electrically conductive cotton samples were produced

based on conductive polymer and graphene, which were denoted as GO-Co, RGO-Co, PPy-Co, and PANI-Co, and the prefixed abbreviation represents the type of applied conductive materials. The schematic preparation of coated cotton samples is shown in Fig. 1.

### The coating of cotton fabric with GO and RGO

The modified Hummer's method was used to synthesize graphene oxide (GO) sheets (Hummers and Offeman 1958). The graphite powder (2 g) and sodium nitrate (2 g) were added to 96 mL of sulfuric

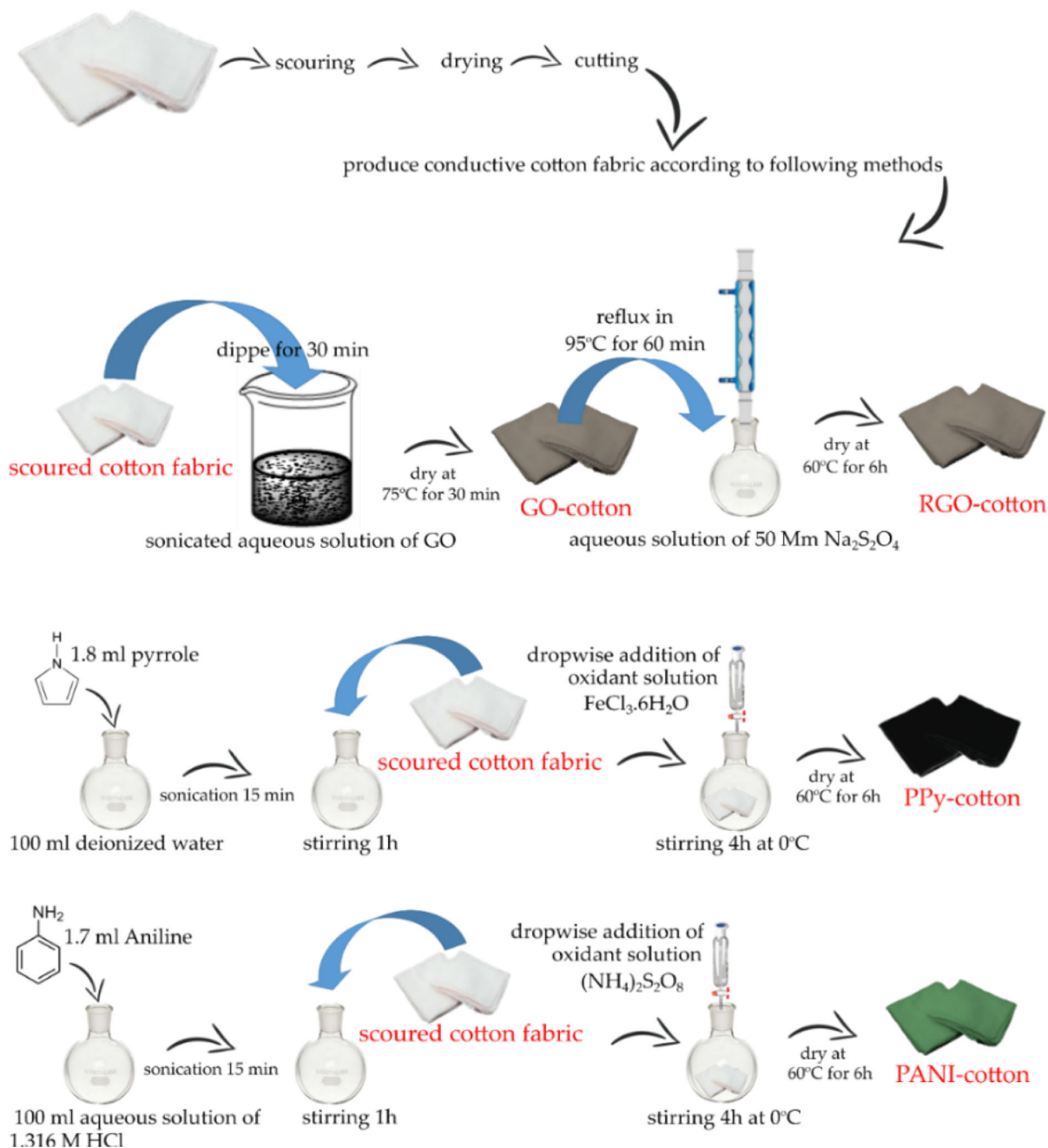


**Fig. 1** Schematic process method for the preparation of conductive cotton samples

acid in a Round-bottom flask (1000 mL), which was in an ice bath (0–5 °C) and stirred continuously (Fig. 1). The stirring was followed for 2 h at this temperature, and 12 g of potassium permanganate was added to this mixture very slowly while carefully controlling the reaction temperature lower than 10 °C. After that, this mixture was stirred at 35 °C for 6 h. The reaction system was immersed in an ice bath (0–5 °C), and then 400 mL %2 H<sub>2</sub>O<sub>2</sub> was added to this mixture very slowly by which changed color to bright brown. The above mixture was refluxed at 98 °C for 30 min, which gave a black-colored solution and was kept under stirring for 24 h at room temperature. Then 400 mL HCl (%5) was added to the above mixture and stirred for 30 min. The resulting mixture was washed repeatedly with deionized water and centrifuged at 3000 rpm several times until it became neutral. After that, an aqueous dispersion of graphite oxide was sonicated for 4 h at 60 °C to exfoliate it to GO. Finally, GO dispersion was freeze-dried for 72 h, which gave the GO powder.

Cotton fabrics were coated with GO as described elsewhere (Shateri-Khalilabad and Yazdanshenas 2013) with some minor modifications. In a typical procedure, an aqueous dispersion of GO (1 mg/mL) with a liquor to goods ratio of 50:1 was prepared using an ultrasonic bath homogenizer for 30 min. The cotton fabrics (5 × 5 cm) were dipped into the prepared dispersion at room temperature for 30 min and then dried at 75 °C for 30 min. The coating process was repeated 20 times to increase GO adsorption. The resulting GO-coated fabrics were referred to as GO (1%w/v)–Cotton.

The GO-coated fabrics (1 g of each) were immersed in a 100 mL aqueous solution of 50 mM Na<sub>2</sub>S<sub>2</sub>O<sub>4</sub>. The mixture was refluxed at 95 °C for 60 min under constant stirring. The resulting fabric was washed with a large amount of deionized water multi times to eliminate the unreacted reducing agents. Finally, the samples were dried at 60 °C for 6 h (Fig. 1). The resulting RGO-coated fabrics were referred to as RGO (1%w/v)–Cotton. The above steps were repeated for different concentrations of GO dispersion, which including 2, 3, 4 and 5 mg/mL, to investigate the effect of concentration of GO dispersion on the electrical conductivity of the coated sample.

### *The coating of cotton fabric with polypyrrole*

The pyrrole was polymerized as an in situ method on cotton fabric in different pyrrole to oxidant molar ratios and monomer quantities (Table 1). In a typical procedure, 1.8 mL pyrrole was dissolved in deionized water (100 mL) in a Round-bottom flask (250 mL), then homogenized by a bath-sonicator. Two cotton fabric samples (5 × 5 cm) were dipped into the prepared solution and kept under gentle stirring at room temperature for 60 min to allow adsorption of pyrrole on the cotton fabrics (Fig. 1). The reaction system was then placed in an ice bath (0 up to 5 °C) and kept under stirring for 15 min. The oxidant solution containing 17 g FeCl<sub>3</sub>·6H<sub>2</sub>O was dissolved in 50 mL deionized water (pyrrole to oxidant molar ratio of 1:2.5) while magnetically stirred at room temperature for 15 min. The steady and dropwise addition of oxidant solution into the reaction system resulted in beginning the polymerization reaction on the surface of cotton fabric. After that, the color of the coated fabric immediately altered from white to black. The reaction was followed for 4 h, and then the coated fabrics were washed with plenty of deionized water for removing unreacted oxidant and monomer alongside unbound PPy. The available and unbound polypyrrole was carefully separated, washed with deionized water, and dried at 60 °C for 6 h for further studies. Finally, the coated fabrics were dried in an oven at 60 °C for 6 h before measurements were performed.

The different concentration of pyrrole (0.25, 0.5, 1 and 1.8) and aniline (0.25, 0.5, 1, 1.7 and 2) was used for modification of cotton fabric. Moreover, FeCl<sub>3</sub>·6H<sub>2</sub>O and (NH<sub>4</sub>)<sub>2</sub>S<sub>2</sub>O<sub>8</sub> were used as an oxidant for in situ polymerizations of Pyrrole and Aniline monomer, respectively. Also, HCl was used as a dopant in the polymerization of aniline monomer.

### *The coating of cotton fabric with Polyaniline*

The in situ polymerization of polyaniline on the cotton fabric was carried out in different aniline: dopant (HCl) molar ratios and quantities of aniline (Table 1). In a typical procedure, 1.7 mL aniline was added to 100 mL of 1.316 M HCl (aniline to dopant molar ratio of 1:7) in a Round-bottom flask (250 mL), then homogenized by bath-sonicator for 15 min (Fig. 1). Two cotton fabric samples (5 × 5 cm) were dipped into the prepared solution and kept under gentle

**Table 1** The description of sample code and the in situ polymerization conditions on the cotton fabric

Monomer	Monomer quantity (mL)	Oxidant molar ratio	Dopant molar ratio	Sample code
Pyrrole	1.8	1:2.5	–	PPy(1.8/1:2.5)-Co
	1.8	1:1	–	PPy(1.8/1:1)-Co
Aniline	1.7	1:1	1:7	PANI(1.7/1:7)-Co
	1.7	1:1	1:1	PANI(1.7/1:1)-Co

stirring at room temperature for 60 min to allow adsorption of aniline on the cotton fabrics. The reaction system was then placed in an ice bath (0 up to 5 °C) and kept under stirring for 15 min. The oxidant solution was prepared by dissolving 4.286 g of  $(\text{NH}_4)_2\text{S}_2\text{O}_8$  in 50 mL deionized water (aniline to oxidant molar ratio of 1:1) and magnetically stirred for 15 min at room temperature. The steady and dropwise addition of oxidant solution into the reaction system resulted in beginning the polymerization reaction on the surface of cotton fabric. After that, the reaction was followed for 4 h, and the color of the fabric samples was altered to green. Then, the coated fabrics were washed with plenty of deionized water for removing unreacted oxidant, monomer, and unbound PANI. The available and unbound polyaniline was carefully separated, washed with deionized water, and dried at 60 °C for 6 h for further studies. Finally, the coated fabrics were dried at 60 °C for 6 h before measurements were performed.

#### Characterization of coated cotton fabric

The Fourier Transform Infrared (FTIR) spectra of each sample were recorded on a Bruker Tensor-27 spectrometer (Germany). The Attenuated Total Reflectance-Fourier Transform Infrared (ATR-FTIR) spectra were collected on a Bruker Equinox-55 spectrometer (Germany). The spectra were analyzed in the wavelength range of 400 and 4000  $\text{cm}^{-1}$ . The morphology of each coated cotton sample was observed using Scanning Electron Microscope (TESCAN MIRA3 XMU, Czech Republic), which was equipped with a field emission gun (FESEM). The crystallographic structure of synthesized conductive materials and coated samples was determined using an X-ray diffractometer (Panalytical X'PertPro, Netherlands) with  $\text{CuK}\alpha$  radiation ( $\lambda = 1.5404 \text{ \AA}$ ). The x-ray diffraction (XRD) pattern of samples was recorded

over the range  $5^\circ \leq 2\theta \leq 90^\circ$  with a step size of  $0.05^\circ$  and a step time of 1 s. The crystallographic parameters of samples were calculated based on the following equations:

$$d = \frac{n\lambda}{2\sin\theta} \text{ (Bragg's law)}, \quad L = \frac{k\lambda}{\beta \cos\theta},$$

$$\text{(Scherrer equati)}, \quad \text{and} \quad N = \frac{L}{d} + 1$$

where  $d$  is the inter-layer spacing,  $L$  is crystallite size,  $N$  is the number of graphene layers in the crystal,  $n$  is a positive integer ( $n = 1$ ),  $\lambda$  is the wavelength of the incident wave ( $\lambda = 0.15404 \text{ nm}$ ),  $\theta$  is the diffraction peak position ( $^\circ$ ),  $k$  is a form factor ( $k = 0.91$ ), and  $\beta$  is the width at half-height of the corresponding diffraction peak in radian. The point-to-point surface resistance of the cotton fabrics was measured according to IEC 61,340–4–10, employing a TERA OHM METER electrical resistivity Test Instrument (Iran) at 22 °C, and 35% relative humidity. The Test Instrument has been calibrated by the NACI laboratory (Certification No. 98L 1307–1/1) according to the IDS-GDL-0316 standard. Moreover, the measurement of out-of-range values, the DEC digital multimeter (model DEC330FC), was coupled with the Test Instrument. The sheet resistance of cotton sample ( $\Omega/\text{square}$ ) was calculated as  $(O \times W/D)$  with  $O$  = electrical resistance of cotton sample in Ohm,  $W$  = width of the sample in cm, and  $D$  = distance between two-point probe in cm. The distance between the probes was adjusted by 1 cm, and each sample was tested 10 times. The color characteristics of prepared conductive cotton fabric were determined using a Ci60, X-Rite spectrophotometer. The reflectance spectrum of each sample was recorded over a range of 400–700 nm, and the color values ( $L^*$ ,  $a^*$ ,  $b^*$ ,  $C^*$ ,  $h^*$ ) were determined under illuminant  $D_{65}$  and the  $10^\circ$  standard observer. Also, the color strength (K/S) of each coated sample was calculated based on the

reflectance spectrum, according to the  $(1 - R)^2/2R$ , in which  $R$  is the reflectance of the sample.

## Results and discussions

The in situ preparation was used to produce the different types of conductive cotton fabric samples via a reduction reaction process on the deposited GO on the coated cotton fabric or polymerization of monomer on the surface of cotton fabric by immersing fabric sample in the reaction mixture of polymerization. The prepared samples were characterized by using different methods, and the obtained results are as a following.

### Morphology of synthesized samples

The SEM images of fibers reveal a typical morphology of cotton fibers, which was modified by different conductive materials. It is clear from the FESEM micrographs (Fig. 2), which no impurity appeared on the surface of pristine cotton fibers and presented relatively smooth and neat surfaces with no mentionable features like rumples or wrinkles (Barani 2014a, 2014b; Barani and Boroumand 2016; Haji et al. 2013). The smooth surface of cotton fabric was altered to a rough surface after modification with conductive materials, such as GO, RGO, PPy, and PANI (Fig. 2). After the coating, a laminar layer of GO appeared on the surface of cotton, which indicates the successful deposition of GO nanosheets on the surface of cotton fibers (Drewniak et al. 2016; Krishnamoorthy et al. 2013; Shojaeenezhad et al. 2017). The GO nanosheets were adsorbed on the surface of cotton fiber due to hydrogen bond and van der Waals' force between functional groups of GO and cotton fiber (Xu et al. 2015; Yu et al. 2011). After that, the GO nanosheets were converted to RGO nanosheets by a reduction method. The RGO nanosheets remained on the cotton fibers surface after the GO nanosheets chemical reduction with  $\text{Na}_2\text{S}_2\text{O}_4$ , which may be due to the homogeneous coating of the GO nanosheets over the cotton fibers. As it is evident from EFSEM images (Fig. 2), the size and morphology of RGO nanosheets are as same as the deposited GO nanosheets on the surface of the cotton fiber after being reduced in the reduction process.

In the case of PPy-coated cotton fabric, polypyrrole formed a continuous layer consisted of spherical particles of different sizes on the surface of cotton fibers, which would enhance its electrical conductivity. Moreover, the coating of cotton fabric through in situ chemical polymerization of aniline resulted in the forming of a layer of HCl-doped granular polyaniline (emeraldine form of polyaniline) over the cotton fibers surface, which eventually would impart electrical conductivity to the cotton fabric.

### FTIR analysis

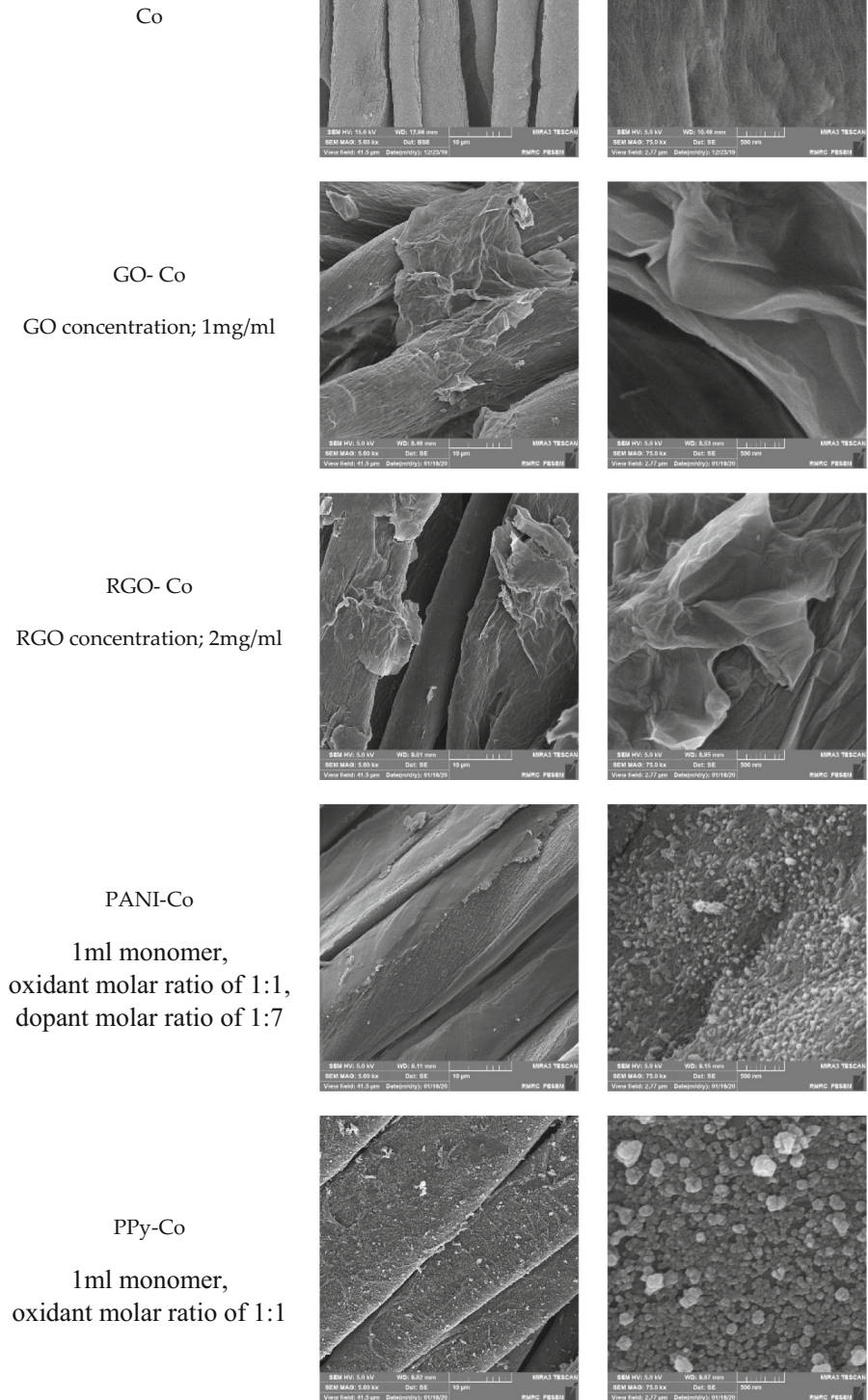
The chemical structure of prepared samples was investigated for evaluating the characteristics of the synthesized conductive materials (GO, RGO, PPy, and PANI) alongside their interaction with the cotton fibers as a textile substrate. The FTIR spectra of the synthesized GO sample (Fig. 3) shows some characteristic signals, which are around 1736 (C=O stretching vibration), 1619 (C=C stretches from un-oxidized aromatic CC bonds), 1226 (C–O stretching vibrations of C–OH from alcohol groups), and  $1055\text{ cm}^{-1}$  (C–O stretching vibrations of C–O–C). The presence of signals assignable to the oxygen-containing functional groups confirmed that the oxidation reaction as a chemical exfoliation was successfully carried out on the graphite. Moreover, there is broadband around  $3404\text{ cm}^{-1}$  due to the OH stretching vibrations of introduced hydroxyl and carboxyl groups of GO and absorbed water molecules between GO sheets. The FTIR spectra of synthesized GO samples agree with other studies (Aliyev et al. 2019; Habte et al. 2019; Krishnamoorthy et al. 2013; Rabchinskii et al. 2018; Romero et al. 2018).

As can be seen, the FTIR spectrum of synthesized PANI shows some characteristic bands as follow; broadband centered around  $3439\text{ cm}^{-1}$  is attributed to the N–H vibrations of PANI. The two absorption peaks at  $1471\text{ cm}^{-1}$  and  $1578\text{ cm}^{-1}$  are assigned to the C = C stretching vibration for the benzenoid and quinonoid ring-stretching vibrations of polyaniline, respectively (Fig. 4a). Moreover, the band at  $1110\text{ cm}^{-1}$  is assigned to the C–N stretching mode for the benzenoid ring, and the presence of a signal at  $789\text{ cm}^{-1}$  is attributed to the C–H vibration (Butoi et al. 2017; Kang et al. 1998; Sariciftci et al. 1987).

In the FTIR spectra of synthesized polypyrrole, the presence of several weak absorption bands in the range



**Fig. 2** Scanning electron microscopy (SEM) of coated cotton fabrics by conductive materials with different magnification (left) 5 kx, and (right) 75 kx



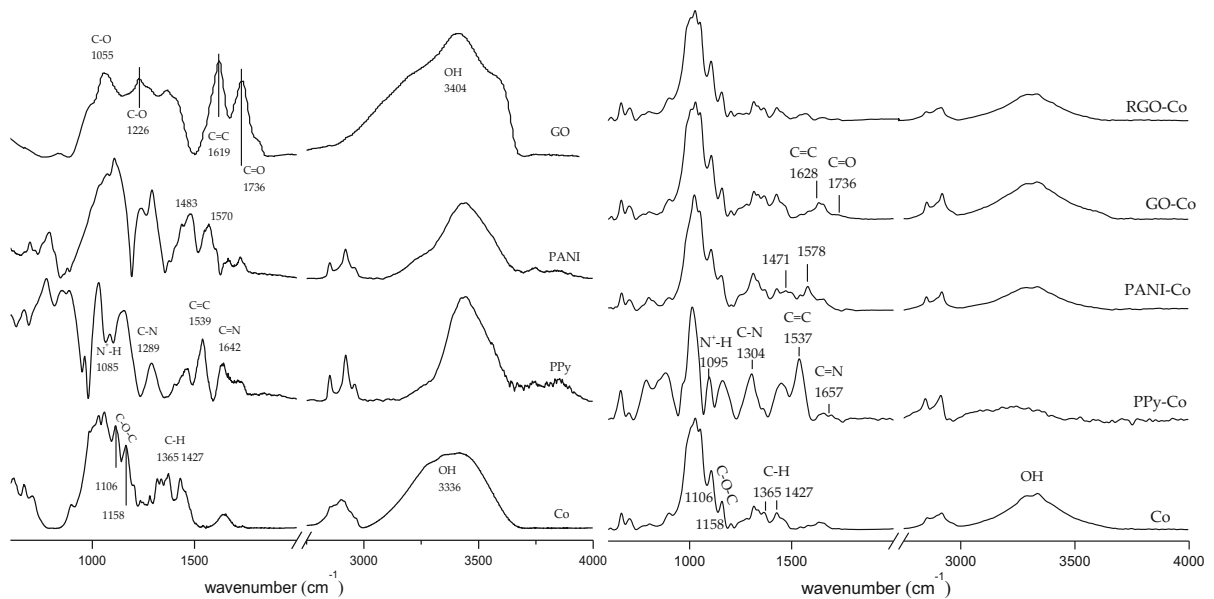


**Fig. 3** Normalized FTIR spectra of (left) cotton and synthesized conductive material and (right) the normalized ATR–FTIR spectra of coated cotton fabric with conductive material (GO–Co with 1 mg/mL GO concentration; RGO–Co with 1 mg/

mL RGO concentration; PANI–Co with 1 mL monomer, oxidant molar ratio of 1:1, and dopant molar ratio of 1:7; PPy–Co with 1 mL monomer, oxidant molar ratio of 1:1). The spectra were normalized based on the highest band intensity

of 1200–1700  $\text{cm}^{-1}$  is associated with the fundamental vibrations of the polypyrrole ring (Fig. 4b). The bands at 1289, 1445, 1539 and 1642  $\text{cm}^{-1}$  are due to the C–N, C=C, C–C, and C=N stretching vibrations of the pyrrole ring. Moreover, the two absorption peaks at 1023 and 1085  $\text{cm}^{-1}$  are attributed to the C–H and N–H in-plane deformation vibrations. The bands that appeared at 2923 and 3432  $\text{cm}^{-1}$  are due to C–H and N–H stretching vibration of polypyrrole, respectively (Kato et al. 1991; Moosvi et al. 2016; Ramesan 2013).

As can be seen, the cotton fiber presents some characteristics in the FTIR and ATR–FTIR spectra (Fig. 3), which are the same and in good agreement with the literature (Barani 2014a, 2014b; Barani and Mahltig 2020; Chung et al. 2004). The FTIR and ATR–FTIR spectra of cotton fiber show some characteristics bands as follow; the characteristics absorption bands of cotton fiber appear in the range from 900 to 1500  $\text{cm}^{-1}$  due to C–O and C–H vibration. A weak peak occurred at 1650  $\text{cm}^{-1}$  due to the O–H bending mode of the adsorbed water molecule. Moreover, a broad peak appeared at around 3400  $\text{cm}^{-1}$  due to the stretching vibration of the hydrogen-bonded O–H in cellulose molecules. By comparing the ATR–FTIR spectra of coated cotton fabric (Fig. 3), it shows that all samples presented the same prominent resonance

bands of cotton fiber and respective coated material. In the ATR–FTIR spectra of GO and RGO-coated cotton fabrics, only characteristic peaks of cotton fiber are visible, which might be due to the low adsorption of GO/RGO on the cotton surface (with a weight gain in the range of approximately 0.72% in RGO(1 M)-cotton and 3.21% in RGO(5 M)-cotton). The ATR–FTIR spectrum of PANI-coated cotton sample presented dominant characteristic peaks of cotton with two absorption peaks at 1471 and 1578  $\text{cm}^{-1}$  attributed to the benzenoid (N–B–N) and quinonoid (N=Q=N) ring-stretching vibrations of polyaniline, respectively. In the ATR–FTIR spectrum of PPy-coated cotton, characteristic peaks of polypyrrole are more prominent due to the high adsorption of polypyrrole on the cotton surface and a high-thickness and uniform layer of polypyrrole. The coating of cotton fabric with PPy and PANI resulted in a lower intensity of the attributed hydroxyl bands around 3400  $\text{cm}^{-1}$  due to hydrogen bonds forming between the hydroxyl groups of cotton fibers and the coated conductive polymer (Fig. 4c). The protonated coated polymer can interact with the functional hydroxyl of cotton fibers and result in the lower intensity (PPy-cotton = – 62% and PANI-cotton = – 38%) of the hydroxyl bands in coated cotton fabric samples.

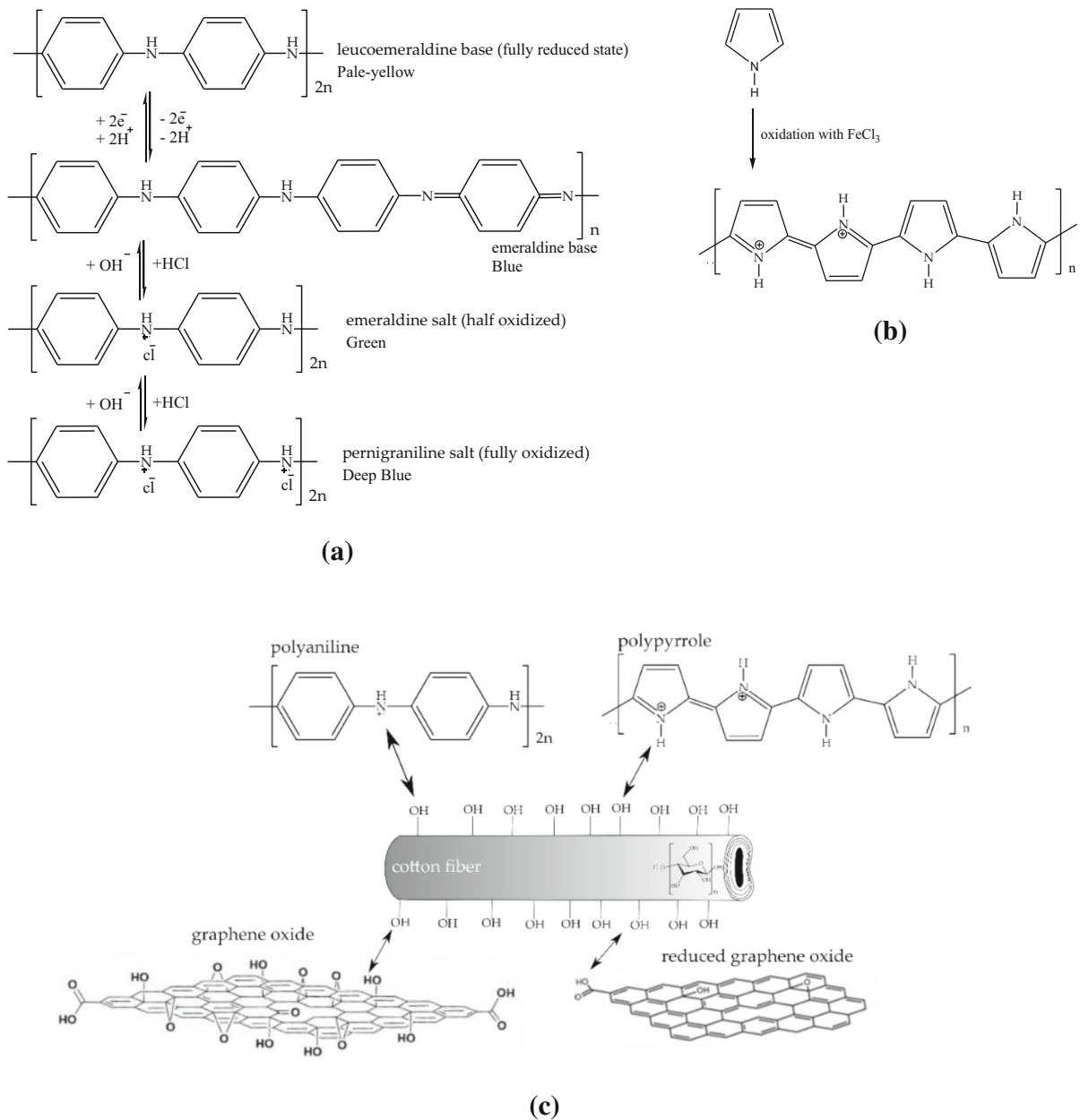


**Fig. 4** The different forms of **a** polyaniline with various oxidation degree, **b** polymerization and chemical structure of Polypyrrole, and **c** the schematic design of hydrogen bonds formed between the hydroxyl groups of cotton fibers and the deposited conductive materials

However, these interactions can enhance the fastness of coated cotton fabric.

#### XRD analysis

This technique was used to determine the average interlayer spacing and the orientation of a single

crystal or grain. Cotton fabric presented some broad reflections peaks due to its semi-crystalline cellulosic structure (Fig. 5) and generally appeared near to the  $2\theta$  angles of  $14.8^\circ$ ,  $16.8^\circ$  and  $22.2^\circ$ , and which are associated to (1–10), (110), and (200) (French 2014; French and Santiago Cintrón 2013). According to XRD diffraction patterns, the position of these

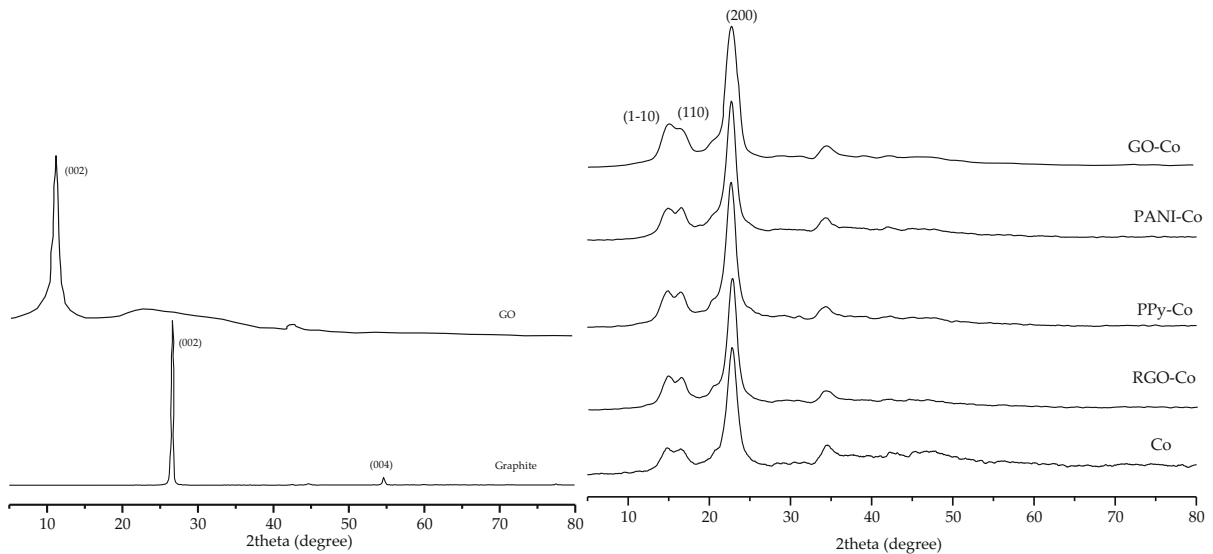


**Fig. 5** The XRD patterns of (left) graphite and synthesized graphene oxide and (right) coated cotton fabric with conductive material

characteristic peaks did not markedly shift after coating conductive material over the cotton fabric sample, and the same results have been reported for the graphene coating over the other textile substrates (Fugetsu et al. 2010; Karimi et al. 2014, 2016; Molina et al. 2015; Nooralian et al. 2016). The characteristic reflection peaks of the graphene will not be distinguishable at the XRD pattern if it is successfully exfoliated and uniformly deposited on the fiber surface (Fugetsu et al. 2010; Karimi et al. 2016; Nooralian et al. 2016; Tang et al. 2014). Moreover, no detectable changes in the XRD pattern of coated cotton fabric might be due to the low quantity of coating materials (GO, RGO, PPy, and PANI) (Karimi et al. 2014; Molina et al. 2015). According to the FESEM images (Fig. 2) of this assay, can confirm that no detecting the characteristic reflection peaks at XRD pattern could be due to the successful exfoliation and uniform deposition on the surface of cotton fibers.

The diffraction pattern of pure graphite powder (Fig. 5) presented an intense peak around  $2\theta = 26.6^\circ$ , which is indexed to (002) crystal plane orientation (Ganguly et al. 2011; Herzog et al. 1994; Hishiyama and Nakamura 1995; Kelly and Billups 2013) with an interlayer spacing of 0.33 nm (Table 2). The exfoliation of graphite intercalation compounds as a top-down process is one of the routes to produce graphene (Eswaraiah et al. 2011; Lee et al. 2019). It is carried out to achieve the desired number of graphene layers.

The graphite exfoliation is performed via a chemical or mechanical method (Wu et al. 2009). The oxidation reaction (Guerrero-Contreras and Caballero-Briones 2015; Muzyka et al. 2018; Sohail et al. 2017) as a chemical exfoliation was used in this assay. After the oxidation reaction, the characteristic peak of graphite (002) is found to be shifted for graphene oxide to around  $2\theta = 11.1^\circ$  (Ganguly et al. 2011; Ju et al. 2010; Ma et al. 2017). The oxidation reaction increased the interlayer spacing (142%) from 0.33 to 0.79 nm due to oxygen-containing functional groups between the layers and water molecules located in the interlayer galleries. Furthermore, the existence of a very small peak around  $2\theta = 42^\circ$  in the XRD pattern of graphene oxide confirms the presence of unordered graphite layers, which is known as a turbostratic disorder structure and is formed due to incomplete oxidation (Chen et al. 2011; Jurkiewicz et al. 2018; Li et al. 2007). The results indicate that the crystallite size,  $L_{002}$ , decreases after oxidation reaction, which might be due to the breaking of crystallites and formation of defects crystal (Hontoria-Lucas et al. 1995; Krishnamoorthy et al. 2013; Romero et al. 2018). Moreover, the oxidation increased the interlayer spacing due to oxygen-containing functional groups, including carbonyl, hydroxyl, and epoxide. The appearance of these functional groups resulted in a decrease in the interactions between the graphene layers by increasing the interlayer distance (Guerrero-Contreras and

**Table 2** The crystallographic parameters of graphite and graphene oxide samples based on the calculation of the XRD pattern

Sample	2 $\theta$ (°) (002) peak	FWHM (°) (002) peak	L <sub>002</sub> (nm)	d <sub>002</sub> (nm)	N
G	26.6100	0.2460	33.1803	0.334675	100
GO	11.0969	0.4428	18.0239	0.796587	23

Caballero-Briones 2015; Romero et al. 2018). Also, the oxidation process resulted in a lower number of graphene layers (Romero et al. 2018) with a 77% reduction in N value (Table 2).

### Electrical conductivity

The sheet resistance of fabric was determined by the two-point probe method, and the obtained data are presented in Fig. 6. The pristine cotton fabric was not an electroconductive textile substrate due to its high electrical resistance ( $1.9 \times 10^{12} \Omega/\text{square}$ ). After deposition of graphene oxide over the cotton sample, the electrical resistance of the GO-Cotton sample presented only a partial decrease. The structure changes of carbon atoms during the oxidation process resulted in a low electrical conductivity of GO. The electrical conductivity of GO dramatically decreased when the oxygen content exceeded (Morimoto et al. 2016; Park et al. 2014; Phiri et al. 2018). The coating of cotton fabric with GO didn't change electrical resistance due to the lack of an extended-conjugated orbital system in GO. But, removing the oxygen-containing functional groups of GO resulted in restoring the original  $sp^2$  electronic structure of carbon atoms and recovering its electrical conductivity. Therefore, the reduction of graphene oxide resulted in enhancing the electrical conductivity of RGO (Karimi et al. 2014; Park et al. 2014). According to this, the reduction of Go to RGO through chemical reduction with  $\text{Na}_2\text{S}_2\text{O}_4$ , the RGO(1%w/v)-Cotton showed a sheet resistance of  $11.5 \times 10^3 \Omega/\text{square}$ , which represented a decrease of 99% compared with GO(1%w/v)-Cotton. The RGO concentration on the coated fabric surface has a considerable effect on the conductivity of the coated cotton sample (Fig. 6a). Increasing the concentration of RGO dispersion from 1 to 5 mg/mL resulted in a lower sheet resistance (– 99%), which is probably due to the increasing number of charge carriers on the surface of cotton

fibers and better surface connection of deposited RGO nanosheets.

PPy and PANI inherently are conducting polymers due to the  $\pi$ -conjugated structure (Fig. 6), which can conduct electrical charges (Varesano et al. 2013). The chemical polymerization of pyrrole is a useful method for producing the conductive substrate in an aqueous solution. Usually, the chemical polymerization of the pyrrole monomer is initiated using ferric chloride as an oxidant. Therefore, the effect of pyrrole to oxidant molar ratio (1 and 2.5) and quantity of pyrrole monomer (0.25, 0.5, 1 and 1.8 mL) was investigated on the electrical conductivity of the PPy-coated cotton sample. It is evident that the pyrrole to oxidant molar ratio has no effect on the conductivity of coated cotton fabric and did not alter the electrical resistance values of cotton fabric (Fig. 6b). However, the monomer quantity having a considerable impact on electrical conductivity. Increasing the monomer quantity from 1 to 1.8 mL resulted in markedly higher electrical resistance (Fig. 6c). This can be related to the accumulation of charge carriers on the surface of cotton fibers, which decreased the charge carrier mobility and disrupted the charge transfer process through charge carriers. Moreover, increasing the monomer quantity would decrease cotton flexibility and softness, which is related to the weight gain of cotton (5% weight gain for PPy(0.25)-Cotton and 32% weight gain for PPy(2)-Cotton) as a result of increasing the degree of polypyrrole adsorption on the cotton surface. Also, decreasing the monomer quantity to 0.25 mL had no significant influence on sheet resistance, and only a little change was observed.

Polyaniline usually is synthesized by chemical polymerization of aniline in an acidic aqueous solution of oxidant. The influence of aniline to dopant molar ratio (1 and 7) and quantity of aniline monomer (0.25, 0.5, 1 and 1.7 mL) was studied on the electrical conductivity of PANI-coated cotton fabric. The results confirm that the sheet resistance of coated cotton

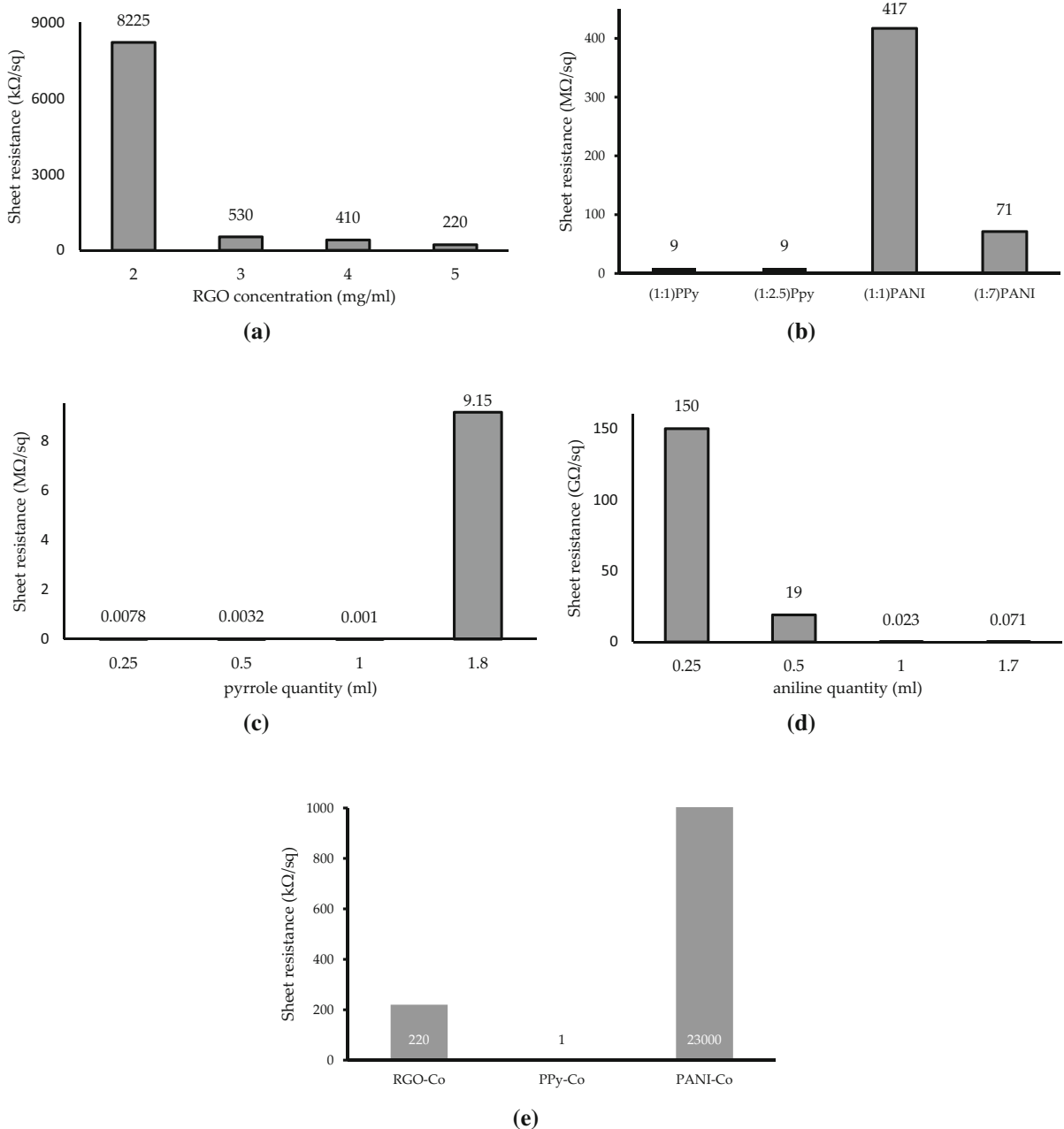


**Fig. 6** The sheet resistance of coated cotton fabric at **a** different RGO concentrations, **b** different molar ratio of oxidant for PPy and dopant for PANI polymerization, **c** different concentration of pyrrole, **d** different concentration of aniline, **e** different

conductive materials at their lowest sheet resistance value [RGO (5 mg/mL), PPy (1 mL monomer, and oxidant molar ratio of 1:1), and PANI (1 mL monomer, oxidant molar ratio of 1:1, dopant molar ratio of 1:7)]

fabrics depends on the molar ratio of aniline to dopant (Fig. 6b). It is evident from the data that an increase of aniline to dopant molar ratio from 1 to 7 resulted in lower sheet resistance of coated sample (from  $417 \times 10^6$  to  $71 \times 10^6 \Omega/\text{square}$ ;  $-83\%$ ). The

pristine cotton fabric presented a low electrical conductivity ( $1.9 \times 10^{12} \Omega/\text{square}$ ), while in situ polymerization of PANI (0.25 mL) on the surface of cotton fabric resulted in a significant decrease ( $150 \times 10^9 \Omega/\text{square}$ ;  $-92\%$ ) in the sheet resistance.

The monomer quantity has a remarkable effect on cotton fabric conductivity (Fig. 6d). Among of different monomer concentrations used, 1 ml of aniline provided the lowest sheet resistance value ( $23 \times 10^6 \text{ M}\Omega/\text{square}$  for aniline to dopant molar ratio of 1:7), which is significantly lower than that of pristine cotton fabric. The lower quantity of aniline monomer ( $< 1 \text{ mL}$ ) resulted in marked increases in the sheet resistance value of the coated sample. The 0.25 mL of aniline monomer presented a higher sheet resistance value than the greater concentration (0.5, 1 and 1.7 mL). The less electrical conductivity at the low quantity of aniline monomer could be attributed to the decrease of doping level (and subsequently the number of charge carriers) on the surface of cotton fibers, which resulted from the reduction of dopant concentration in the reaction medium. Although increasing the monomer quantity up to 1.7 and 2 mL had no significant influence on sheet resistance, only a little change was observed. The electrical conductivity of synthesized polyaniline is very sensitive to the applied polymerization conditions. The only protonated emeraldine is a form of conducting polyaniline (Ansari 2006; Balint et al. 2014; Boeva and Sergeev 2014; Wallace et al. 2008), which is synthesized by oxidative polymerization of aniline in aqueous acid. The emeraldine salt could be formed using 1 ml of aniline monomer with aniline to dopant molar ratio of 1:7. The color coordination results confirmed the emeraldine synthesis on this sample by the appearance of green color (Fig. 4a). Bajgar et al. (2016) has reported the deposition of conducting polymers (polyaniline or polypyrrole) on cotton fabric as electrodes to collect the electrical response to the stimulation of a Venus flytrap plant. They reported that the coating with PPy provided a lower sheet resistance value compared with PANI, which is in agreement with the obtained results in the current study. The lowest electrical resistance ( $1 \times 10^3 \Omega/\text{square}$ ) was obtained for PPy(1 ml)-Cotton sample, which represents a decrease of approximately 91% and 99% compared with RGO(1%w/v)-Cotton and PANI (1 mL)-Cotton samples, respectively (Fig. 6e).

#### Colorimetric characteristics of coated cotton fabric

The effect of conductive materials on the color appearance of coated samples was studied by measuring the color values ( $L^*$ ,  $a^*$ ,  $b^*$ , and  $h^\circ$ ). The

difference in the color of coated fabrics is quite distinguishable with the naked eye. The color value of coated samples indicates that their color is brown, dark brown, black, green, and dark blue (Fig. 7). When the cotton fabric treated with graphene oxide (GO), the color of pristine cotton altered from white to brown due to the brownish color of deposited GO on the surface of cotton fibers (Fig. 7a). Also, the reduction of GO to RGO through chemical reduction, the RGO (1%w/v)-Cotton represents a lower chromaticity and lightness value than GO (1%w/v)-Cotton. Moreover, the higher concentration of RGO results in a lower chromaticity value.

The PPy-coated cotton samples represent a black color with the lowest chromaticity and lightness value. The coating cotton fabric with polyaniline shows various colors from green to blue, which is different from the other coated samples. The PANI-cotton samples with different polyaniline content presented a hue angle between  $179^\circ$  and  $244^\circ$  (Fig. 7b), which confirms the appearance of green and blue color-coated cotton fabric (polyaniline content from 0.25 to 2 mL). The polyaniline polymer represents different colors due to various degrees of oxidation and protonation. When the leucoemeraldine as a fully reduced polymer is oxidized, the two forms of fully oxidized (pernigraniline) and half oxidized polymer (emeraldine) are formed (Fig. 4a). Therefore, the color of different forms of the synthesized polyaniline polymer indicates the degree of its oxidation. The various steps of oxidation polymerization are associated with color changes. The protonated pernigraniline presented a blue color and was altered to a green color due to the emeraldine salt.

The different lightness and color strength of the coated cotton fabric (Fig. 7c) indicates the deposition of different GO or RGO concentrations on the textile substrate. Increasing graphene concentrations, more and more graphene was embedded in the cotton fibers, resulted in a dark brown fabric with higher color strength. Among of different conductive materials used, the polypyrrole provided the highest color strength (Fig. 7d), which is significantly greater compared to the other coated cotton samples (GO-cotton, RGO-cotton, and PANI-cotton). Moreover, the results confirm that the color strength of polypyrrole coated cotton fabrics was affected by pyrrole content (Fig. 7b). Applying 2 ml of pyrrole monomer resulted in the lowest color strength and presented the highest

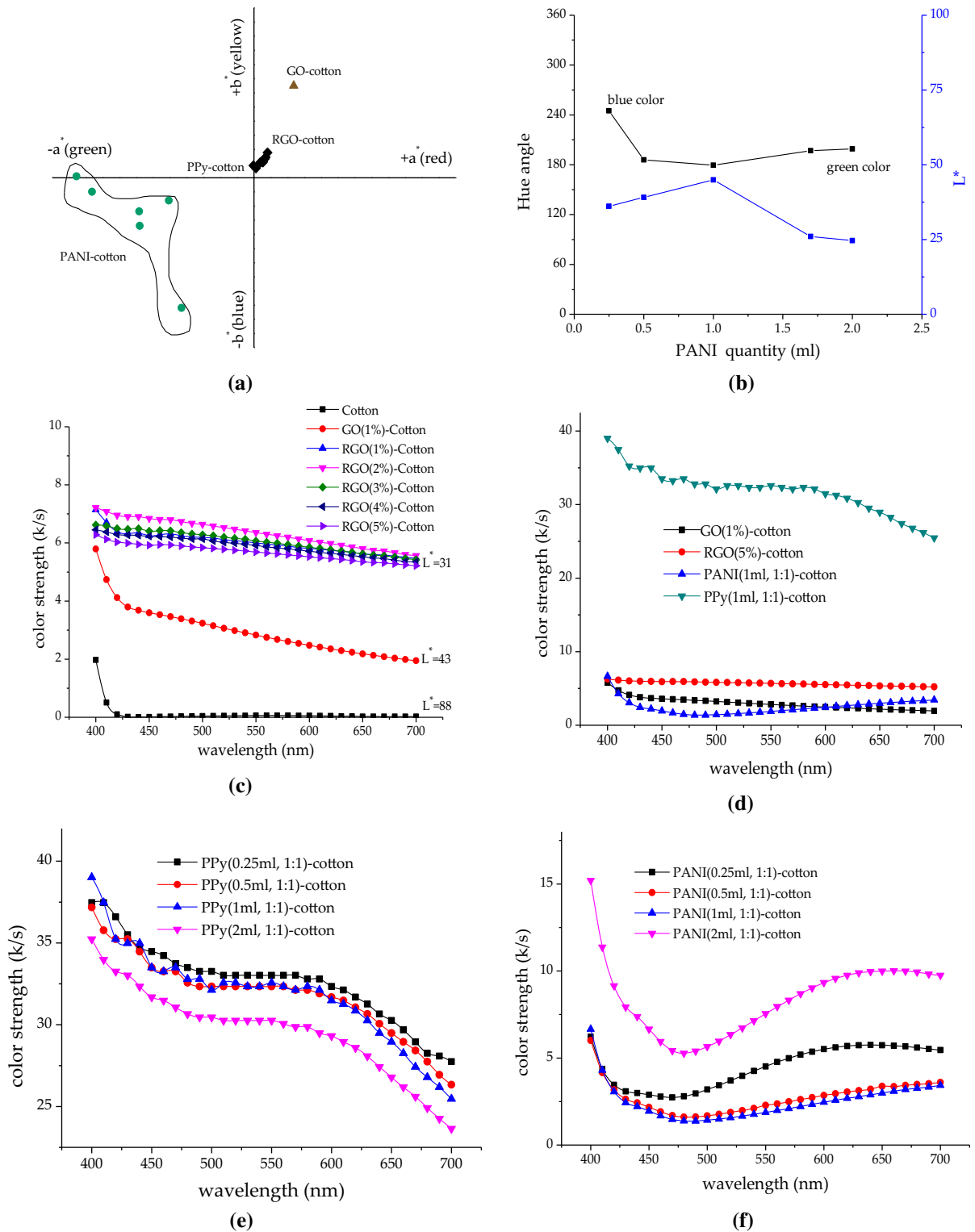


**Fig. 7** The color characteristics of coated cotton samples with conductive materials such as **a** color coordination, **b** hue angle at CIELAB color space, and **c–f** reflectance spectra



sheet resistance among of used quantity of monomer. Therefore, the color strength of polyaniline-coated cotton fabrics depends on the aniline content (Fig. 7f). Its trend is as same as sheet resistance values of polyaniline coated samples versus of aniline content. The lowest color strength of polyaniline-coated cotton fabric is achieved using the 1 mL of pyrrole monomer. This pyrrole quantity (1 mL) is presented the lowest sheet resistance due to the formation of emeraldine salt.

## Conclusions

The electrical conductivity of cotton fabrics was enhanced using an in situ approach, such as polymerization of conductive polymer or synthesis of reduced graphene oxide. The prepared samples were characterized by using different methods. The size and morphology of RGO nanosheets were as same as the deposited GO nanosheets on the surface of cotton fibers. The synthesis of polypyrrole and polyaniline resulted in a continuous layer on the cotton fiber surface, which eventually imparted electrical conductivity to the cotton fabric. The FTIR spectroscopy showed the excellent production of synthesized conductive materials. The ATR–FTIR spectroscopy confirmed the presence of hydrogen bonds between the hydroxyl groups of cotton fibers and the conductive materials. The coating of conductive material over the cotton fabric did not markedly shift the position of XRD characteristic peaks, which could be due to the successful exfoliation of synthesized graphene and their uniform deposition.

The pristine cotton fabric is not an electroconductive textile substrate due to its high electrical resistance ( $1.9 \times 10^{12} \Omega/\text{square}$ ). The deposition of graphene oxide as a coating on the cotton fabric resulted in a partial decrease in the electrical resistance. The reduction of graphene oxide resulted in enhancing the electrical conductivity of RGO ( $220 \times 10^3 \Omega/\text{square}$ ), which represented a decrease of 95% compared with the GO–Cotton sample. The PPy (1 mL)–Cotton showed the lowest sheet resistance of  $1 \times 10^3 \Omega/\text{square}$ , representing a decrease of approximately 99% compared with RGO (1%w/v)–Cotton sample. The sheet resistance value of polyaniline coated cotton fabrics depended on the molar ratio of aniline to oxidant and was very sensitive to the

degree of oxidation and protonation. The protonated pernigraniline showed a blue color which was later altered to the green color due to the emeraldine salt and provided the lowest sheet resistance.

## Declaration

**Conflict of interest** The authors have no conflict of interest to declare.

**Ethical approval** This article does not contain any studies with human participants or animals performed by any of the authors.

## References

- Ahmed H, Khattab TA, Mashaly HM, El-Halwagy AA, Rehan M (2020) Plasma activation toward multi-stimuli responsive cotton fabric via in situ development of polyaniline derivatives and silver nanoparticles. *Cellulose* 27:2913–2926. <https://doi.org/10.1007/s10570-020-02980-7>
- Al-Oqla FM, Sapuan SM, Anwer T, Jawaid M, Hoque ME (2015) Natural fiber reinforced conductive polymer composites as functional materials: a review. *Synth Met* 206:42–54. <https://doi.org/10.1016/j.synthmet.2015.04.014>
- Alamer FA (2018) Structural and electrical properties of conductive cotton fabrics coated with the composite polyaniline/carbon black. *Cellulose* 25:2075–2082. <https://doi.org/10.1007/s10570-018-1667-9>
- Aliyev E, Filiz V, Khan MM, Lee YJ, Abetz C, Abetz V (2019) Structural characterization of graphene oxide: surface functional groups and fractionated oxidative debris. *Nanomater Basel* 9(8):1180. <https://doi.org/10.3390/nano9081180>
- Allison L, Hoxie S, Andrew TL (2017) Towards seamlessly-integrated textile electronics: methods to coat fabrics and fibers with conducting polymers for electronic applications. *Chem Commun* 53:7182–7193. <https://doi.org/10.1039/c7cc02592k>
- Ansari R (2006) Polypyrrole conducting electroactive polymers: synthesis and stability studies. *E-J Chem* 3:860413. <https://doi.org/10.1155/2006/860413>
- Bajgar V, Penhaker M, Martinková L, Pavlovič A, Bober P, Trchová M, Stejskal J (2016) Cotton fabric coated with conducting polymers and its application in monitoring of carnivorous plant response. *Sensors* 16(4):498. <https://doi.org/10.3390/s16040498>
- Balint R, Cassidy NJ, Cartmell SH (2014) Conductive polymers: towards a smart biomaterial for tissue engineering. *Acta Biomater* 10(6):2341–2353. <https://doi.org/10.1016/j.actbio.2014.02.015>
- Barani H (2014a) Surface activation of cotton fiber by seeding silver nanoparticles and in situ synthesizing ZnO nanoparticles. *New J Chem* 38:4365–4370. <https://doi.org/10.1039/c4nj00547c>

- Barani H (2014b) Preparation of antibacterial coating based on in situ synthesis of ZnO/SiO<sub>2</sub> hybrid nanocomposite on cotton fabric. *Appl Surf Sci* 320:429–434. <https://doi.org/10.1016/j.apsusc.2014.09.102>
- Barani H, Boroumand MN (2016) Alkaline treatment effect on the properties of in-situ synthesised ZnO nanoparticles on cotton fabric. *IET Nanobiotechnol* 10(3):162–168. <https://doi.org/10.1049/iet-nbt.2015.0048>
- Barani H, Mahltig B (2020) Using microwave irradiation to catalyze the in-situ manufacturing of silver nanoparticles on cotton fabric for antibacterial and UV-protective application. *Cellulose* 27(15):9105–9121. <https://doi.org/10.1007/s10570-020-03400-6>
- Bhadra J, Alkareem A, Al-Thani N (2020) A review of advances in the preparation and application of polyaniline based thermoset blends and composites. *J Polym Res* 27(5):122. <https://doi.org/10.1007/s10965-020-02052-1>
- Bharadiya P, Mahajan C, Sharma AK, Mishra S (2019) Enriched mechanical, UV shielding and flame retarding properties of cotton fabric coated with graphite nano platelets filled polyaniline–gum arabic nanocomposites. *Cellulose* 26:8135–8151. <https://doi.org/10.1007/s10570-019-02638-z>
- Boeva ZA, Sergeev VG (2014) Polyaniline: synthesis, properties, and application. *Polym Sci Ser C* 56(1):144–153. <https://doi.org/10.1134/S1811238214010032>
- Butoi B, Groza A, Dinca P, Balan A, Barna V (2017) Morphological and structural analysis of polyaniline and poly(o-anisidine) layers generated in a DC glow discharge plasma by using an oblique angle electrode deposition configuration. *Polym Basel* 9(12):732. <https://doi.org/10.3390/polym9120732>
- Chen L, Xu Z, Li J, Min C, Liu L, Song X, Chen G, Meng X (2011) Reduction and disorder in graphene oxide induced by electron-beam irradiation. *Mater Lett* 65:1229–1230. <https://doi.org/10.1016/j.matlet.2011.01.063>
- Chen W, Yan L, Bangal PR (2010) Chemical reduction of graphene oxide to graphene by sulfur-containing compounds. *J Phys Chem C* 114(47):19885–19890. <https://doi.org/10.1021/jp107131v>
- Chung C, Lee M, Choe E (2004) Characterization of cotton fabric scouring by FT-IR ATR spectroscopy. *Carbohydr Polym* 58(4):417–420. <https://doi.org/10.1016/j.carbpol.2004.08.005>
- David NC, Anavi D, Milanovich M, Popowski Y, Frid L, Amir E (2017) Preparation and properties of electro-conductive fabrics based on polypyrrole: covalent vs non-covalent attachment. *Mater Sci Eng* 254:032002. <https://doi.org/10.1088/1757-899X/254/3/032002>
- Drewniak S, Muzyka R, Stolarczyk A, Pustelny T, Kotyczka-Morańska M, Setkiewicz M (2016) Studies of reduced graphene oxide and graphite oxide in the aspect of their possible application in gas sensors. *Sensors* 16(1):103. <https://doi.org/10.3390/s16010103>
- Eswaraiah V, Jyothirmayee Aravind SS, Ramaprabhu S (2011) Top down method for synthesis of highly conducting graphene by exfoliation of graphite oxide using focused solar radiation. *J Mater Chem* 21(19):6800–6803. <https://doi.org/10.1039/c1jm10808e>
- French AD (2014) Idealized powder diffraction patterns for cellulose polymorphs. *Cellulose* 21(2):885–896. <https://doi.org/10.1007/s10570-013-0030-4>
- French AD, Santiago Cintrón M (2013) Cellulose polymorphy, crystallite size, and the segal crystallinity index. *Cellulose* 20:583–588. <https://doi.org/10.1007/s10570-012-9833-y>
- Fugetsu B, Sano E, Yu H, Mori K, Tanaka T (2010) Graphene oxide as dyestuffs for the creation of electrically conductive fabrics. *Carbon* 48(12):3340–3345. <https://doi.org/10.1016/j.carbon.2010.05.016>
- Ganguly A, Sharma S, Papakonstantinou P, Hamilton J (2011) Probing the thermal deoxygenation of graphene oxide using high-resolution in situ X-ray-based spectroscopies. *J Phys Chem C* 115(34):17009–17019. <https://doi.org/10.1021/jp203741y>
- Gao WW, Zhang GX, Zhang FX (2015) Enhancement of flame retardancy of cotton fabrics by grafting a novel organic phosphorous-based flame retardant. *Cellulose* 22:2787–2796. <https://doi.org/10.1007/s10570-015-0641-z>
- Gholampour A, Valizadeh Kiamahalleh M, Tran DNH, Ozbakkaloglu T, Losic D (2017) From graphene oxide to reduced graphene oxide: impact on the physiochemical and mechanical properties of graphene-cement composites. *ACS Appl Mater Interface* 9(49):43275–43286. <https://doi.org/10.1021/acsami.7b16736>
- Guerrero-Contreras J, Caballero-Briones F (2015) Graphene oxide powders with different oxidation degree, prepared by synthesis variations of the Hummers method. *Mater Chem Phys* 153:209–220. <https://doi.org/10.1016/j.matchemphys.2015.01.005>
- Habte AT, Ayele DW, Hu M (2019) Synthesis and characterization of reduced graphene oxide (rGO) started from graphene oxide (GO) using the tour method with different parameters. *Adv Mater Sci Eng* 2019:5058163. <https://doi.org/10.1155/2019/5058163>
- Haji A, Barani H, Qavamnia SS (2013) In situ synthesis and loading of silver nanoparticles on cotton fabric. *Ind Textila* 64(1):8–12
- He S, Chen Z, Xin B, Zhang F, Wang X, Liu Y, Peng A, Yang Y (2019a) Surface functionalization of Ag/polypyrrole-coated cotton fabric by in situ polymerization and magnetron sputtering. *Text Res J* 89:4884–4895. <https://doi.org/10.1177/0040517519842801>
- He X, Song P, Shen X, Sun Y, Ji Z, Zhou H, Li B (2019b) Chitosan-assisted synthesis of wearable textile electrodes for high-performance electrochemical energy storage. *Cellulose* 26:9349–9359. <https://doi.org/10.1007/s10570-019-02727-z>
- Herzog B, Bokern D, Braun T, Schloegl R, Troyer C (1994) On the oxidation of graphite: an in situ XRD-study. *Mater Sci Forum* 166:517–522. <https://doi.org/10.4028/www.scientific.net/MSF.166-169.517>
- Higashimura H (2012) Oxidative Coupling Polymerization. *Polym Sci* 5:141–173. <https://doi.org/10.1016/B978-0-444-53349-4.00136-9>
- Hishiyama Y, Nakamura M (1995) X-ray diffraction in oriented carbon films with turbostratic structure. *Carbon* 33:1399–1403. [https://doi.org/10.1016/0008-6223\(95\)00086-S](https://doi.org/10.1016/0008-6223(95)00086-S)

- Hontoria-Lucas C, López-Peinado AJ, López-González JDD, Rojas-Cervantes ML, Martín-Aranda RM (1995) Study of oxygen-containing groups in a series of graphite oxides: physical and chemical characterization. *Carbon* 33:1585–1592. [https://doi.org/10.1016/0008-6223\(95\)00120-3](https://doi.org/10.1016/0008-6223(95)00120-3)
- Hummers WS, Offeman RE (1958) Preparation of graphitic oxide. *J Am Chem Soc* 80:1339. <https://doi.org/10.1021/ja01539a017>
- Ju HM, Choi SH, Huh SH (2010) X-ray diffraction patterns of thermally-reduced graphenes. *J Korean Phys Soc* 57(6):1649–1652. <https://doi.org/10.3938/jkps.57.1649>
- Jurkiewicz K, Pawlyta M, Burian A (2018) Structure of carbon materials explored by local transmission electron microscopy and global powder diffraction probes. *C J Carbon Res* 4(4):68. <https://doi.org/10.3390/c4040068>
- Kang ET, Neoh KG, Tan KL (1998) Polyaniline: a polymer with many interesting intrinsic redox states. *Prog Polym Sci* 23:277–324. [https://doi.org/10.1016/S0079-6700\(97\)00030-0](https://doi.org/10.1016/S0079-6700(97)00030-0)
- Karimi L, Yazdanshenas ME, Khajavi R, Rashidi A, Mirjalili M (2014) Using graphene/TiO<sub>2</sub> nanocomposite as a new route for preparation of electroconductive, self-cleaning, antibacterial and antifungal cotton fabric without toxicity. *Cellulose* 21(5):3813–3827. <https://doi.org/10.1007/s10570-014-0385-1>
- Karimi L, Yazdanshenas ME, Khajavi R, Rashidi A, Mirjalili M (2016) Functional finishing of cotton fabrics using graphene oxide nanosheets decorated with titanium dioxide nanoparticles. *J Text Inst* 107:1122–1134. <https://doi.org/10.1080/00405000.2015.1093311>
- Kato H, Nishikawa O, Matsui T, Honma S, Kokado H (1991) Fourier transform infrared spectroscopy study of conducting polymer polypyrrole: higher order structure of electrochemically synthesized film. *J Phys Chem* 95:6014–6016. <https://doi.org/10.1021/j100168a055>
- Kaur G, Adhikari R, Cass P, Bown M, Gunatillake P (2015) Electrically conductive polymers and composites for biomedical applications. *RSC Adv* 5:37553–37567. <https://doi.org/10.1039/c5ra01851j>
- Ke Q, Wang J (2016) Graphene-based materials for supercapacitor electrodes: a review. *J Materiomics* 2:37–54. <https://doi.org/10.1016/j.jmat.2016.01.001>
- Kelly KF, Billups WE (2013) Synthesis of soluble graphite and graphene. *Acc Chem Res* 46(1):4–13. <https://doi.org/10.1021/ar300121q>
- Kongahge D, Foroughi J, Gambhir S, Spinks GM, Wallace GG (2016) Fabrication of a graphene coated nonwoven textile for industrial applications. *RSC Adv* 6:73203–73209. <https://doi.org/10.1039/c6ra15190f>
- Krishnamoorthy K, Veerapandian M, Yun K, Kim SJ (2013) The chemical and structural analysis of graphene oxide with different degrees of oxidation. *Carbon* 53:38–49. <https://doi.org/10.1016/j.carbon.2012.10.013>
- Le TH, Kim Y, Yoon H (2017) Electrical and electrochemical properties of conducting polymers. *Polym Basel* 9(4):150. <https://doi.org/10.3390/polym9040150>
- Lee J, Noh S, Pham ND, Shim JH (2019) Top-down synthesis of S-doped graphene nanosheets by electrochemical exfoliation of graphite: metal-free bifunctional catalysts for oxygen reduction and evolution reactions. *Electrochim Acta* 313:1–9. <https://doi.org/10.1016/j.electacta.2019.05.015>
- Li ZQ, Lu CJ, Xia ZP, Zhou Y, Luo Z (2007) X-ray diffraction patterns of graphite and turbostratic carbon. *Carbon* 45:1686–1695. <https://doi.org/10.1016/j.carbon.2007.03.038>
- Lou C, Wang S, Liang T, Pang C, Huang L, Run M, Liu X (2017) A graphene-based flexible pressure sensor with applications to plantar pressure measurement and gait analysis. *Materials* 10(9):1068. <https://doi.org/10.3390/ma10091068>
- Ma C, Yang K, Wang L, Wang X (2017) Facile synthesis of reduced graphene oxide/Fe<sub>3</sub>O<sub>4</sub> nanocomposite film. *J Appl Biomater Funct Mater* 15:1–6. <https://doi.org/10.5301/jabfm.5000341>
- Machida S, Miyata S, Techagumpuch A (1989) Chemical synthesis of highly electrically conductive polypyrrole. *Synth Met* 31:311–318. [https://doi.org/10.1016/0379-6779\(89\)90798-4](https://doi.org/10.1016/0379-6779(89)90798-4)
- Malinauskas A (2001) Chemical deposition of conducting polymers. *Polymer* 42(9):3957–3972. [https://doi.org/10.1016/S0032-3861\(00\)00800-4](https://doi.org/10.1016/S0032-3861(00)00800-4)
- Matsuhisa N, Kaltenbrunner M, Yokota T, Jinno H, Kuribara K, Sekitani T, Someya T (2015) Printable elastic conductors with a high conductivity for electronic textile applications. *Nat Commun* 6(1):7461. <https://doi.org/10.1038/ncomms8461>
- Molina J, Fernandes F, Fernández J, Pastor M, Correia A, Souto AP, Carneiro JO, Teixeira V, Cases F (2015) Photocatalytic fabrics based on reduced graphene oxide and TiO<sub>2</sub> coatings. *Mater Sci Eng B Solid* 199:62–76. <https://doi.org/10.1016/j.mseb.2015.04.013>
- Moosvi SK, Majid K, Ara T (2016) Studying the electrical, thermal, and photocatalytic activity of nanocomposite of polypyrrole with the photoadduct of K<sub>3</sub>[Fe(CN)<sub>6</sub>] and diethylenetriamine. *Mater Res* 19(5):983–990. <https://doi.org/10.1590/1980-5373-MR-2015-0786>
- Morimoto N, Kubo T, Nishina Y (2016) Tailoring the oxygen content of graphite and reduced graphene oxide for specific applications. *Sci Rep UK* 6:21715. <https://doi.org/10.1038/srep21715>
- Muthulakshmi B, Kalpana D, Pitchumani S, Renganathan NG (2006) Electrochemical deposition of polypyrrole for symmetric supercapacitors. *J Power Sources* 158:1533–1537. <https://doi.org/10.1016/j.jpowsour.2005.10.013>
- Muzyka R, Drewniak S, Pustelny T, Chrubasik M, Gryglewicz G (2018) Characterization of graphite oxide and reduced graphene oxide obtained from different graphite precursors and oxidized by different methods using Raman spectroscopy. *Materials* 11(7):1050. <https://doi.org/10.3390/ma11071050>
- Nooralian Z, Parvinezadeh Gashti M, Ebrahimi I (2016) Fabrication of a multifunctional graphene/polyvinylphosphonic acid/cotton nanocomposite via facile spray layer-by-layer assembly. *RSC Adv* 6:23288–23299. <https://doi.org/10.1039/c6ra00296j>
- Palza H, Zapata PA, Angulo-Pineda C (2019) Electroactive smart polymers for biomedical applications. *Materials* 12(2):277. <https://doi.org/10.3390/ma12020277>

- Park S, An J, Potts JR, Velamakanni A, Murali S, Ruoff RS (2011) Hydrazine-reduction of graphite- and graphene oxide. *Carbon* 49(9):3019–3023. <https://doi.org/10.1016/j.carbon.2011.02.071>
- Park W, Hu J, Jauregui LA, Ruan X, Chen YP (2014) Electrical and thermal conductivities of reduced graphene oxide/polystyrene composites. *Appl Phys Lett* 104(11):113101. <https://doi.org/10.1063/1.4869026>
- Patil AJ, Deogaonkar SC (2012) A novel method of in situ chemical polymerization of polyaniline for synthesis of electrically conductive cotton fabrics. *Text Res J* 82:1517–1530. <https://doi.org/10.1177/0040517512452930>
- Pei S, Cheng H-M (2012) The reduction of graphene oxide. *Carbon* 50(9):3210–3228. <https://doi.org/10.1016/j.carbon.2011.11.010>
- Peng L, Su B, Yu A, Jiang X (2019) Review of clothing for thermal management with advanced materials. *Cellulose* 26:6415–6448. <https://doi.org/10.1007/s10570-019-02534-6>
- Phiri J, Johansson L-S, Gane P, Maloney T (2018) A comparative study of mechanical, thermal and electrical properties of graphene-, graphene oxide- and reduced graphene oxide-doped microfibrillated cellulose nanocomposites. *Compos Part B-Eng* 147:104–113. <https://doi.org/10.1016/j.compositesb.2018.04.018>
- Rabchinskii MK, Dideikin AT, Kirilenko DA, Baidakova MV, Shnitov VV, Roth F, Konyakhin SV, Besedina NA, Pavlov SI, Kuricyn RA, Lebedeva NM, Brunkov PN, Vul AY (2018) Facile reduction of graphene oxide suspensions and films using glass wafers. *Sci Rep-UK* 8:14154. <https://doi.org/10.1038/s41598-018-32488-x>
- Ramesan MT (2013) Synthesis, characterization, and conductivity studies of polypyrrole/copper sulfide nanocomposites. *J Appl Polym Sci* 128:1540–1546. <https://doi.org/10.1002/app.38304>
- Romero A, Lavin-Lopez MP, Sanchez-Silva L, Valverde JL, Paton-Carrero A (2018) Comparative study of different scalable routes to synthesize graphene oxide and reduced graphene oxide. *Mater Chem Phys* 203:284–292. <https://doi.org/10.1016/j.matchemphys.2017.10.013>
- Sariciftci N S, Neugebauer H, Kuzmany H, Neckel A (1987) In situ FTIR Spectroscopy of Polyaniline. In: Electronic properties of conjugated polymers. Proceedings of an International Winter School, Kirchberg, pp 228–231. [https://doi.org/10.1007/978-3-642-83284-0\\_39](https://doi.org/10.1007/978-3-642-83284-0_39)
- Shateri-Khalilabad M, Yazdanshenas ME (2013) Fabricating electroconductive cotton textiles using graphene. *Carbohydr Polym* 96(1):190–195. <https://doi.org/10.1016/j.carbpol.2013.03.052>
- Shea JJ (1999) Handbook of Conducting Polymers. *IEEE Electric Insul Mag* 15(1):37–37. <https://doi.org/10.1109/MEI.1999.744595>
- Shojaeenezhad SS, Farbod M, Kazeminezhad I (2017) Effects of initial graphite particle size and shape on oxidation time in graphene oxide prepared by Hummers' method. *J Sci Adv Mater Dev* 2:470–475. <https://doi.org/10.1016/j.jsamd.2017.09.003>
- Sohail M, Saleem M, Ullah S, Saeed N, Afridi A, Khan M, Arif M (2017) Modified and improved Hummer's synthesis of graphene oxide for capacitors applications. *Mod Electron Mater* 3(3):110–116. <https://doi.org/10.1016/j.moem.2017.07.002>
- Tang Y, He Z, Mosseler JA, Ni Y (2014) Production of highly electro-conductive cellulosic paper via surface coating of carbon nanotube/graphene oxide nanocomposites using nanocrystalline cellulose as a binder. *Cellulose* 21:4569–4581. <https://doi.org/10.1007/s10570-014-0418-9>
- Tian Z, Yu H, Wang L, Saleem M, Ren F, Ren P, Chen Y, Sun R, Sun Y, Huang L (2014) Recent progress in the preparation of polyaniline nanostructures and their applications in anticorrosive coatings. *RSC Adv* 4(54):28195. <https://doi.org/10.1039/c4ra03146f>
- Varesano A, Rombaldoni F, Tonetti C (2013) Electrically conductive and hydrophobic cotton fabrics by polypyrrole-oleic acid coating. *Fiber Polym* 14:703–709. <https://doi.org/10.1007/s12221-013-0703-5>
- Wallace G G, Teasdale P R, Spinks G M, Kane-Maguire L A P (2008) Conductive electroactive polymers. In: *Conductive electroactive polymers*. CRC Press. <https://doi.org/10.1201/9781420067156>
- Wang C, Guo R, Lan J, Jiang S, Zhang Z (2017) Microwave-assisted synthesis of silver/reduced graphene oxide on cotton fabric. *Cellulose* 24:4045–4055. <https://doi.org/10.1007/s10570-017-1392-9>
- Wong CPP, Lai CW, Lee KM, Abd Hamid SB (2015) Advanced chemical reduction of reduced graphene oxide and its photocatalytic activity in degrading reactive black 5. *Materials* 8(10):7118–7128. <https://doi.org/10.3390/ma8105363>
- Wu Z-S, Ren W, Gao L, Liu B, Jiang C, Cheng H-M (2009) Synthesis of high-quality graphene with a pre-determined number of layers. *Carbon* 47(2):493–499. <https://doi.org/10.1016/j.carbon.2008.10.031>
- Xie J, Pan W, Guo Z, Jiao SS, Ping Yang L (2019) In situ polymerization of polypyrrole on cotton fabrics as flexible electrothermal materials. *J Eng Fiber Fabr* 14:1–8. <https://doi.org/10.1177/1558925019827447>
- Xu LL, Guo MX, Liu S, Bian SW (2015) Graphene/cotton composite fabrics as flexible electrode materials for electrochemical capacitors. *RSC Adv* 5:25244–25249. <https://doi.org/10.1039/c4ra16063k>
- Xue CH, Wu Y, Guo XJ, Liu BY, Di WH, Jia ST (2020) Superhydrophobic, flame-retardant and conductive cotton fabrics via layer-by-layer assembly of carbon nanotubes for flexible sensing electronics. *Cellulose* 27:3455–3468. <https://doi.org/10.1007/s10570-020-03013-z>
- Yang JC, Liao W, Deng SB, Cao ZJ, Wang YZ (2016) Flame retardation of cellulose-rich fabrics via a simplified layer-by-layer assembly. *Carbohydr Polym* 151:434–440. <https://doi.org/10.1016/j.carbpol.2016.05.087>
- Yang M, Fu C, Xia Z, Cheng D, Cai G, Tang B, Wang X (2018) Conductive and durable CNT-cotton ring spun yarns. *Cellulose* 25(7):4239–4249. <https://doi.org/10.1007/s10570-018-1839-7>
- Yu G, Hu L, Vosgueritchian M, Wang H, Xie X, McDonough JR, Cui X, Cui Y, Bao Z (2011) Solution-processed graphene/MnO<sub>2</sub> nanostructured textiles for high-performance electrochemical capacitors. *Nano Lett* 11(7):2905–2911. <https://doi.org/10.1021/nl2013828>

- Yue B, Wang C, Ding X, Wallace GG (2012) Polypyrrole coated nylon lycra fabric as stretchable electrode for supercapacitor applications. *Electrochim Acta* 68:18–24. <https://doi.org/10.1016/j.electacta.2012.01.109>
- Yue B, Wang C, Ding X, Wallace GG (2013) Electrochemically synthesized stretchable polypyrrole/fabric electrodes for supercapacitor. *Electrochim Acta* 113:17–22. <https://doi.org/10.1016/j.electacta.2013.09.024>
- Zhao J, Wu G, Wang P, Wang T, Li Z, Chen L (2019) Mussel-inspired construction of multifunctional cotton fabric with superhydrophobicity, conductivity and antibacterial activity. *Cellulose* 26:6979–6993. <https://doi.org/10.1007/s10570-019-02553-3>
- Zhao Y, Li Y, Kang W, He Y, Liu W, Liu H, Cheng B (2017) A novel flexible sensor for respiratory monitoring based on: in situ polymerization of polypyrrole and polyurethane coating. *RSC Adv* 7:49576–49585. <https://doi.org/10.1039/c7ra08331a>
- Zhou T, Chen F, Liu K, Deng H, Zhang Q, Feng J, Fu Q (2011) A simple and efficient method to prepare graphene by reduction of graphite oxide with sodium hydrosulfite. *Nanotechnology* 22:045704. <https://doi.org/10.1088/0957-4484/22/4/045704>
- Zhou X, Song W, Zhu G (2020) A facile approach for fabricating silica dioxide/reduced graphene oxide coated cotton fabrics with multifunctional properties. *Cellulose* 27:2927–2938. <https://doi.org/10.1007/s10570-020-02990-5>

**Publisher's Note** Springer Nature remains neutral with regard to jurisdictional claims in published maps and institutional affiliations.